

Supporting Information

Nitrogen-doped Porous Carbon Derived from Residuary Shaddock Peels: A Promising and Sustainable Anode for High Energy Density Asymmetric Supercapacitors†

Kang Xiao,^a Liang-Xin Ding,^{*a} Hongbin Chen,^a Suqing Wang,^a Xihong Lu^b and Haihui Wang^{*a}

^aSchool of Chemistry & Chemical Engineering, South China University of Technology, No. 381 Wushan Road, Guangzhou 510640, China;

^bSchool of Chemistry and Chemical Engineering, Sun Yat-Sen University, Guangzhou 510275, China.

S1. Experimental details

Preparation of nitrogen-doped nanoporous carbon: Fresh shaddock peels were first removal the outer yellow epidermis and washed with alcohol, deionized water and dried at 80 °C. Typically, 2.0 g cleaned shaddock peels were soaked in the melamine saturated solution at 90 °C for 10 min. After that, the Shaddock peels contain with melamine was dried at 80 °C for 10 h in a vacuum drying oven. To obtain the nitrogen-doped porous carbon, the as-prepared shaddock peels were annealed in a tubular furnace under an argon atmosphere for 4 h (annealing temperature 600-900 °C, heating rate: 5 °C min⁻¹). The obtained carbonized materials were then washed with 5 M KOH and 2 M HCl to remove the impurities, respectively. The final product (denoted as NPC-*T*, where *T* is the annealing temperature.) were further washed with deionized (DI) water and dried at 70 °C in air. For comparison,

the porous carbon (denoted as PC-700) was annealed at 700 °C under the same steps while without melamine.

Preparation of MnO₂ on Ni foam: MnO₂ was grown on Ni foam by electrodeposition process, the electrodeposition was conducted in 0.02 M Mn(NO₃)₂ and 0.1 M NaNO₃ aqueous solution with a saturated calomel electrode (SCE) served as the reference electrode and platinum as the counter electrode at 1.0 V.

Fabrication of solid-state ASCs: The solid-state MnO₂/NPC-ASC devices were assembled by MnO₂ as the positive electrode and NPC-700 as the negative electrode with a separator and LiCl/PVA gel as a solid electrolyte. The gel electrolyte was prepared by mixing 4.24 g LiCl and 2 g PVA powder in 20 mL deionized water and being heated at 85 °C under vigorous stirring for 2 h. Prior to assembly, the NPC-700, MnO₂ electrodes and separator were immersed in the gel electrolyte, and then assembled together. Finally the device kept at 45 °C for 24 h to remove excess water in the electrolyte.

Materials characterization and electrochemical measurements: The morphologies, structures of the products were characterized by field emission scanning electron microscopy (FE-SEM) (Hitachi S-4800), transmission electron microscopy (TEM) (JEOL 2200FS, 200 kV), X-ray photoelectron spectroscopy (XPS, ESCALAB 250), X-ray diffraction (XRD, Bruker D8 Advance) and Raman spectra (LabRAM Aramis), respectively. The BET specific surface area, total pore volume and pore size distribution were obtained from nitrogen sorption measurements (Micromeritics analyzer ASAP 2010 (USA)). The electrochemical performance of NPC electrodes

were investigated in a conventional three-electrode cell using a CHI760 electrochemical workstation (Chenhua, Shanghai), with a SCE reference electrode and a Pt counter-electrode in 6 M KOH aqueous solution. The working electrode was prepared by mixing 80 wt % active material (about 2 mg), 10 wt % acetylene black, and 10 wt % poly(vinylidene fluoride) (PVDF) in ethanol and coated onto a nickel foam. The as-formed electrodes were dried in vacuum at 80 °C for 12 h.

Calculations:

The specific capacitance is calculated from the discharge curve using the following formula:¹

$$C = \frac{Idt}{mdV}$$

where C is the specific capacitance (F g^{-1}), I is the applied current (A), t is the discharge time (s), m is the mass of the NPC or PC (g), and dV is the applied voltage (V).

The capacitance of $\text{MnO}_2/\text{NPC-ACS}$ is calculated from the discharge curve using the following formula:¹

$$C = \frac{Idt}{mdV}$$

where C is the specific capacitance (F g^{-1}), I is the applied current (A), t is the discharge time (s), m is the totalmass of the NPC and MnO_2 (g), and dV is the applied voltage (V).

The mass ratio between the two electrodes is given by the equation:²

$$\frac{m_{\text{NPC}}}{m_{\text{MnO}_2}} = \frac{C_{\text{MnO}_2}}{C_{\text{NPC}}} \frac{E_{\text{MnO}_2}}{E_{\text{NPC}}}$$

where C is the specific capacitance of NPC and MnO_2 (F g^{-1}), E is the potential range for the charge-discharge process (V).

The power density and energy density were calculated using the following equations:³

$$E = \frac{1}{2}CV^2$$

$$P = \frac{E}{t}$$

where C is the specific capacitance of MnO₂//NPC-ACS (F g⁻¹), t is the discharge time (s)

S2. Supplementary figures and tables

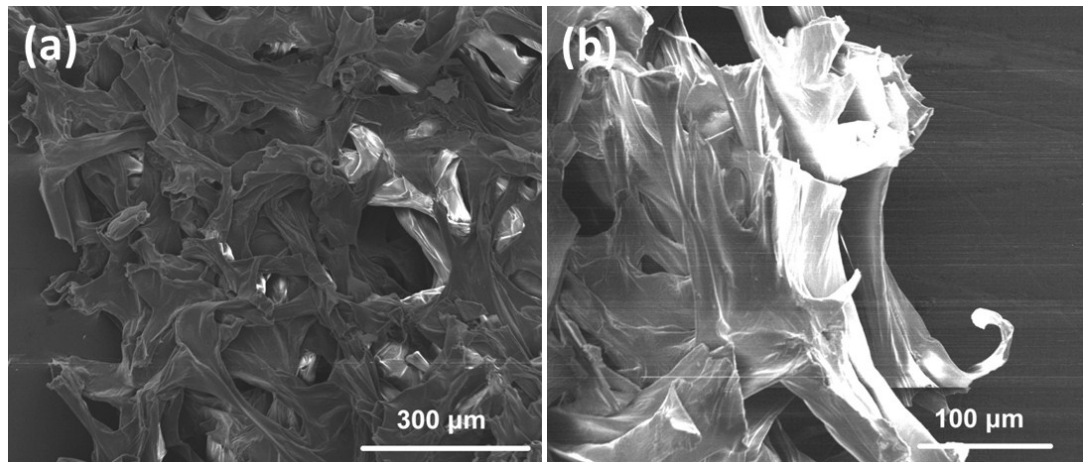


Fig. S1 SEM images of the dried shaddock peels.

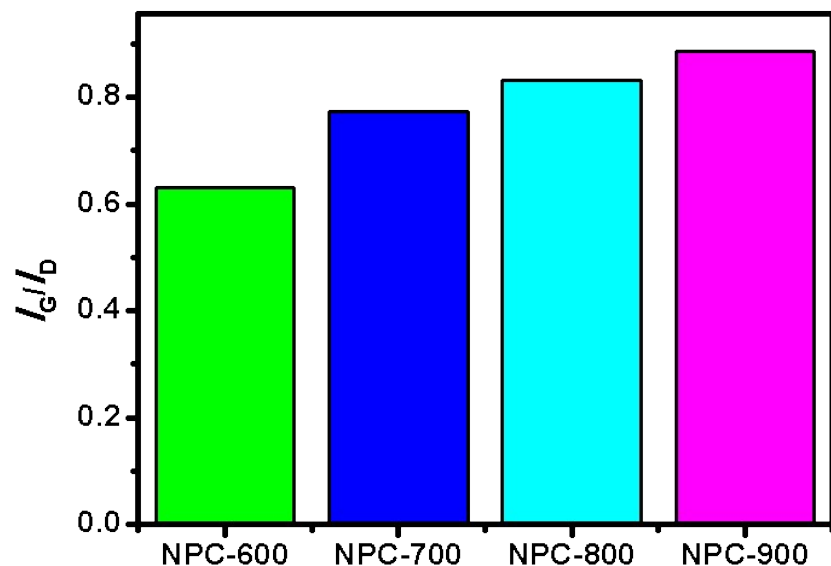


Fig. S2 The ratio of I_G/I_D .

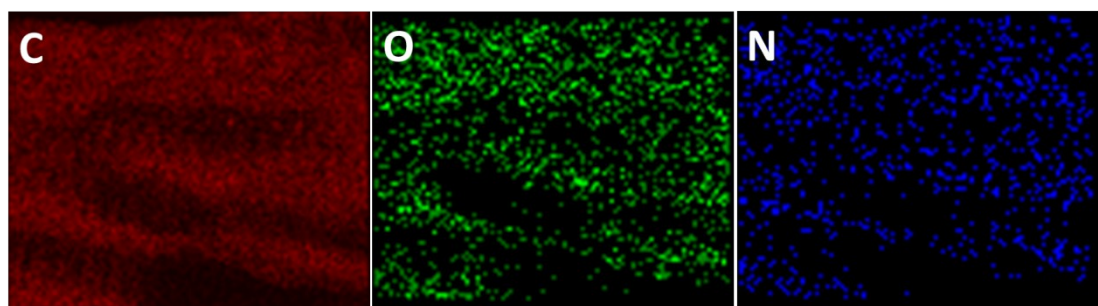


Fig. S3 EELS mapping of carbon, oxygen and nitrogen in NPC-700.

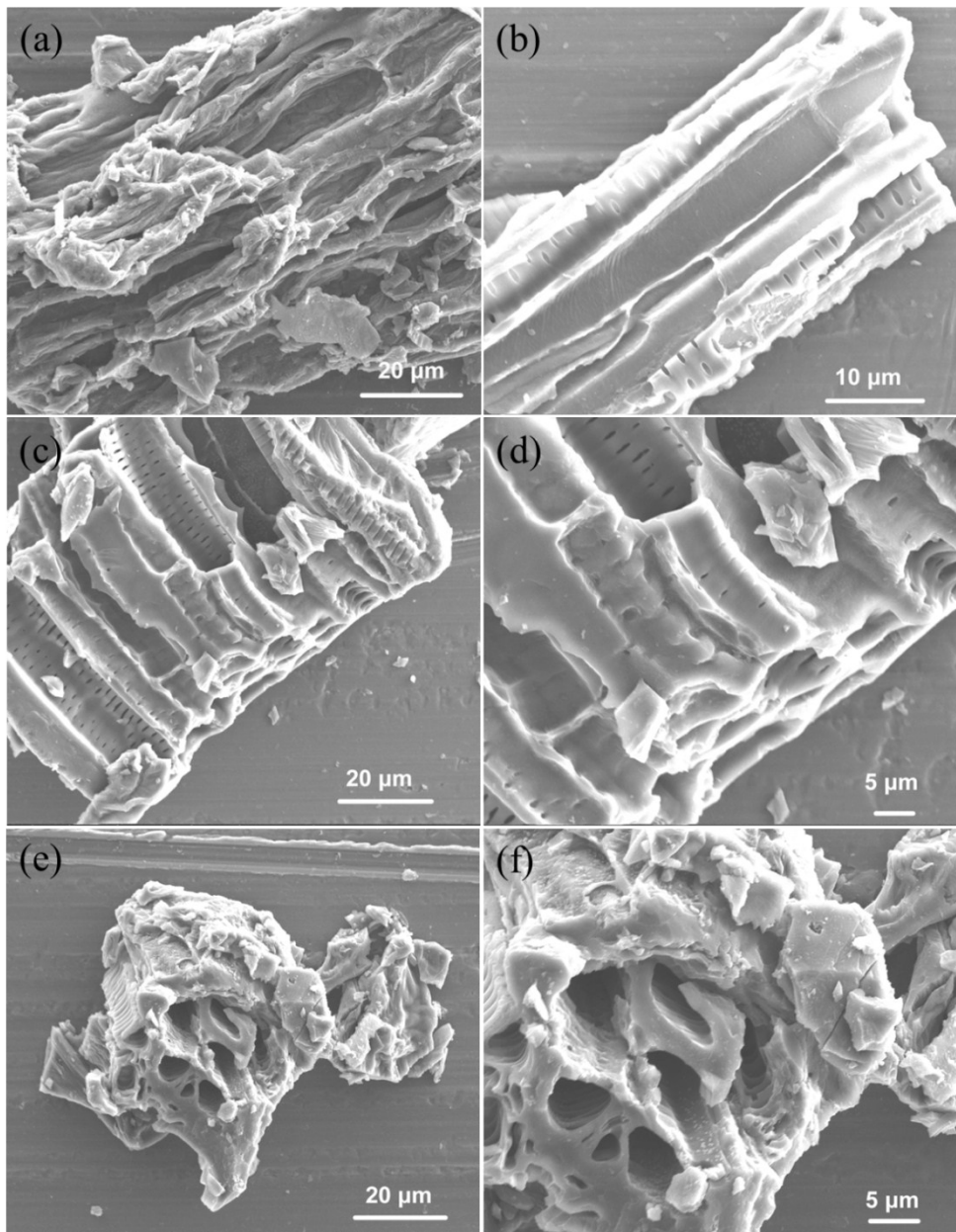


Fig. S4 SEM images of NPC-600 (a-b), NPC-800 (c-d), and NPC-900 (e-f).

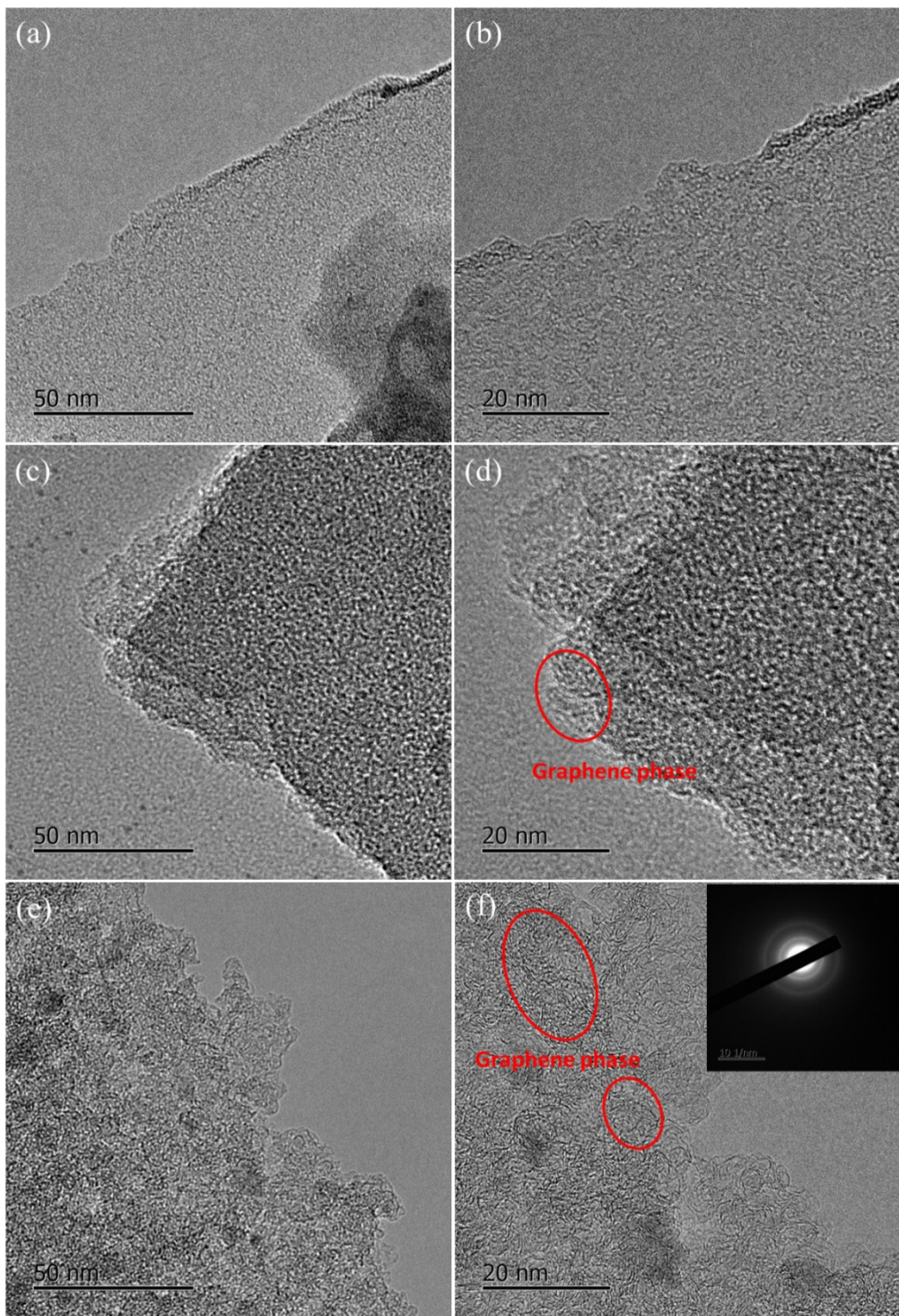


Fig. S5 TEM images of NPC-600 (a-b), NPC-800 (c-d), and NPC-900 (e-f).

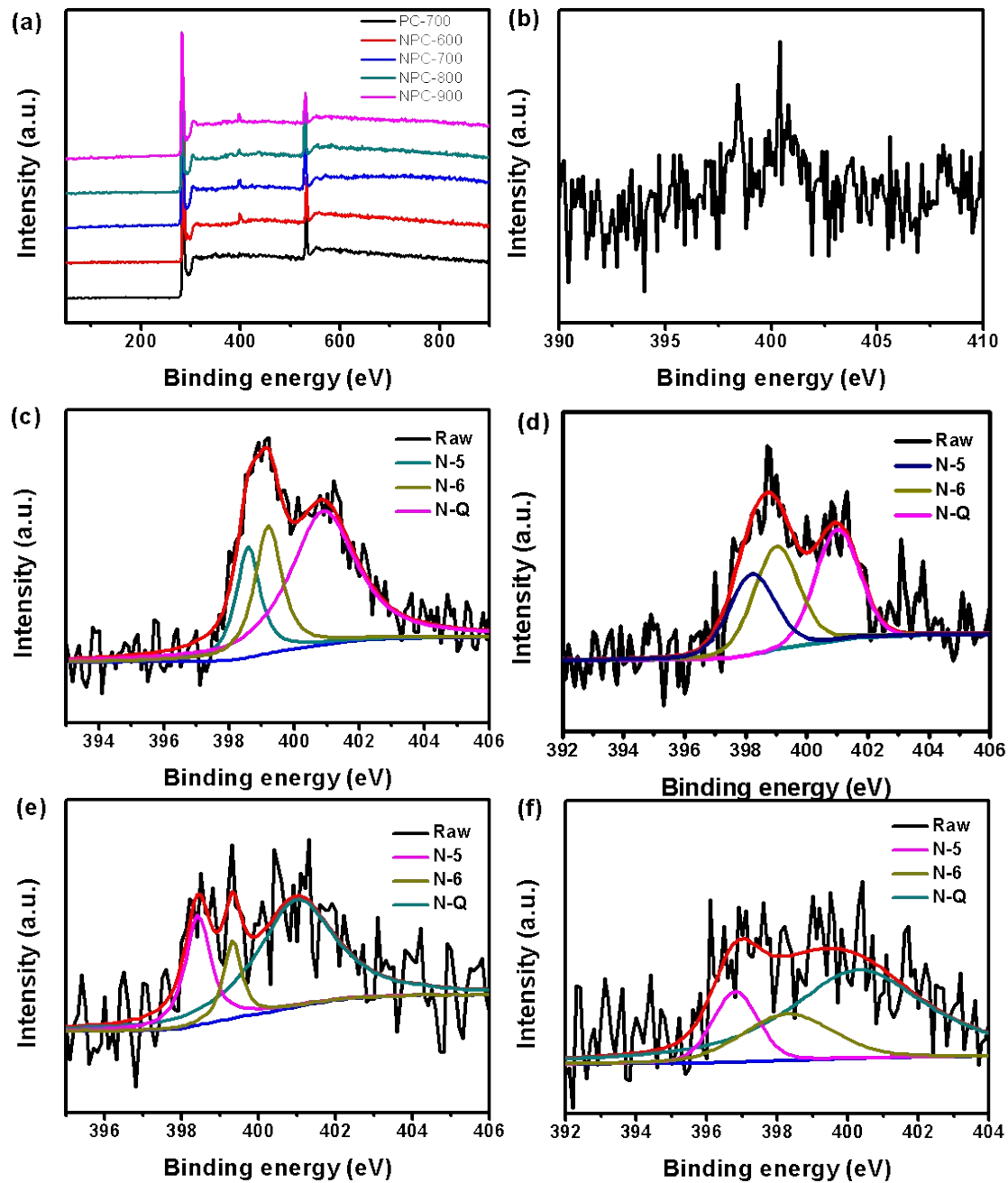


Fig. S6 (a) XPS survey of the all samples. N1s spectrum of PC-700 (b), NPC-600 (c), NPC-700 (d), NPC-800 (e) and NPC-900 (f).

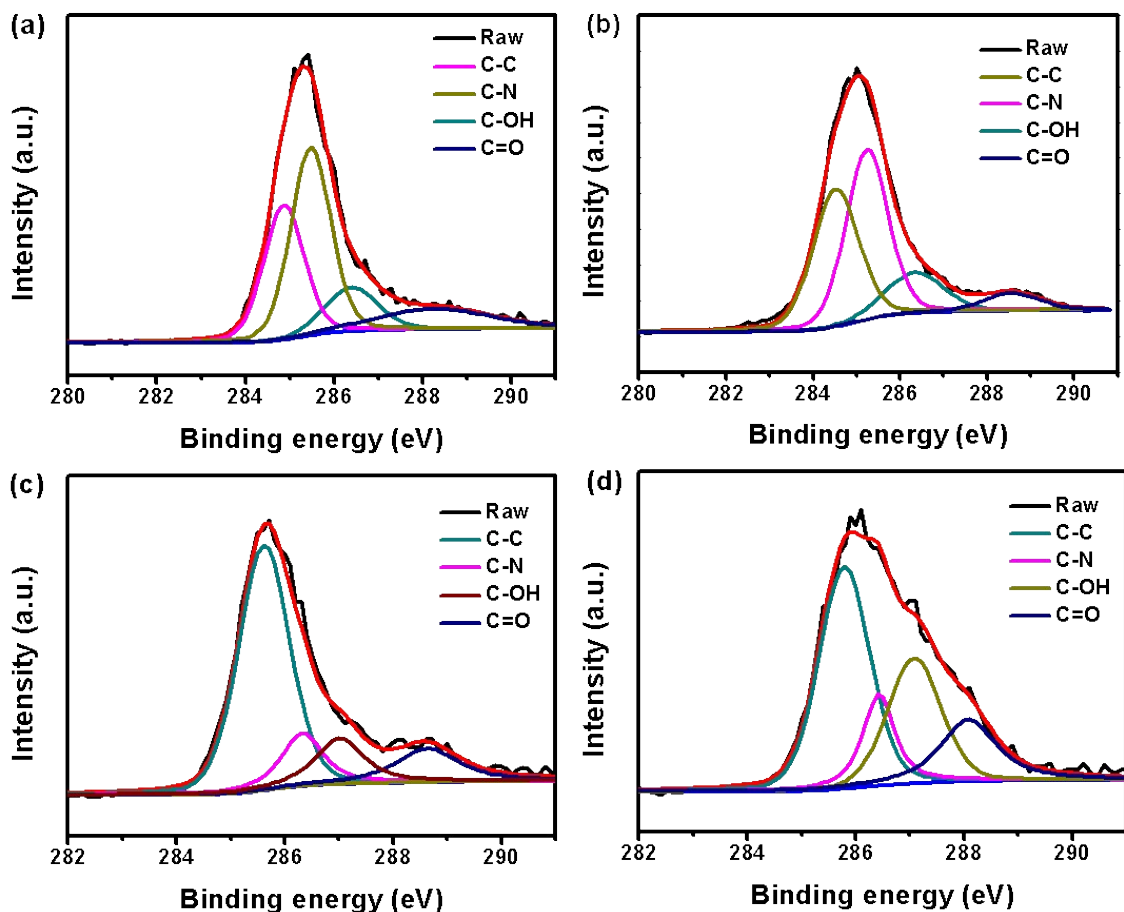


Fig. S7 C1s spectrum of NPC-600 (a), NPC-700 (b), NPC-800 (c) and NPC-900 (d).

Table S1. Relative surface concentrations of carbon and nitrogen species obtained by fitting the C 1s and N1s core level XPS spectra.

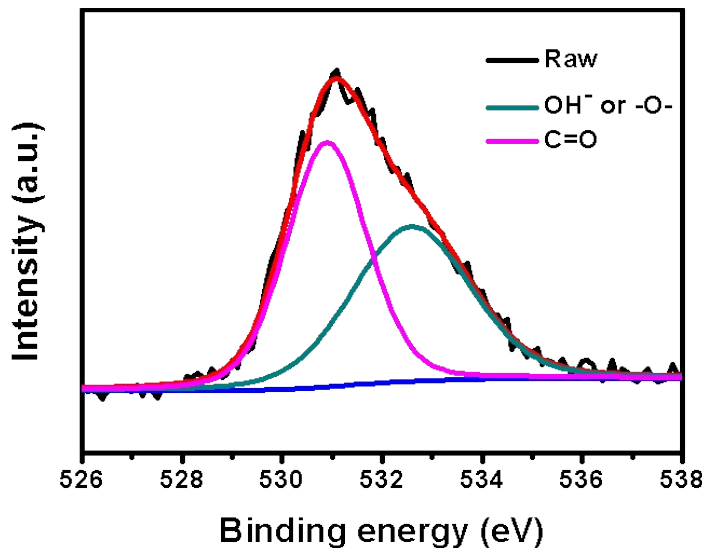


Fig. S8 High-resolution O 1s XPS spectra of NPC-700.

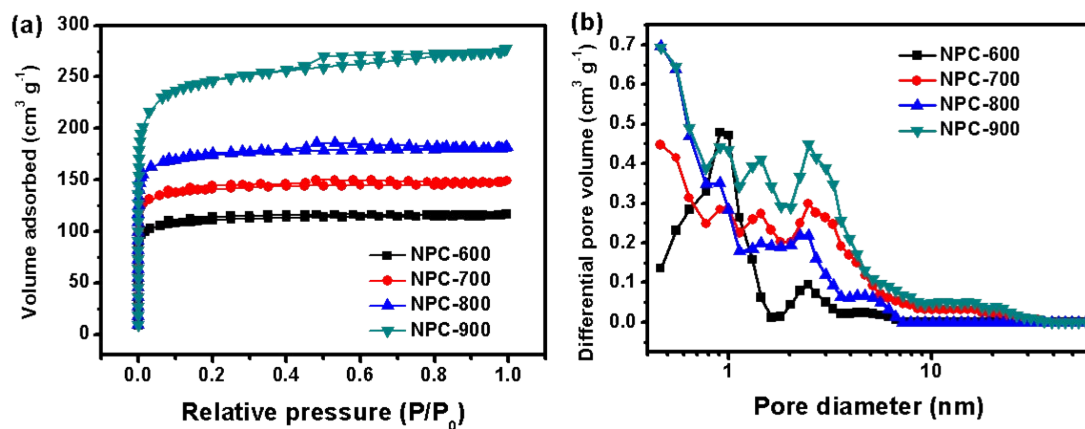


Fig. S9 Nitrogen sorption isotherms (a) and pore size distribution curves (b) of the samples.

Table S2 Textural properties of the shaddock peels derived carbon.

Sample	S_{BET} ($\text{m}^2 \text{ g}^{-1}$)	S_{micro} ($\text{m}^2 \text{ g}^{-1}$)	V_{total} ($\text{cm}^3 \text{ g}^{-1}$)	V_{micro} ($\text{cm}^3 \text{ g}^{-1}$)	V_{meso} ($\text{cm}^3 \text{ g}^{-1}$)
NPC-600	373.4	306.9	0.179	0.14	0.016
NPC-700	474.5	396.3	0.228	0.154	0.053
NPC-800	581.2	485.7	0.279	0.227	0.049
NPC-900	830	601	0.426	0.328	0.082

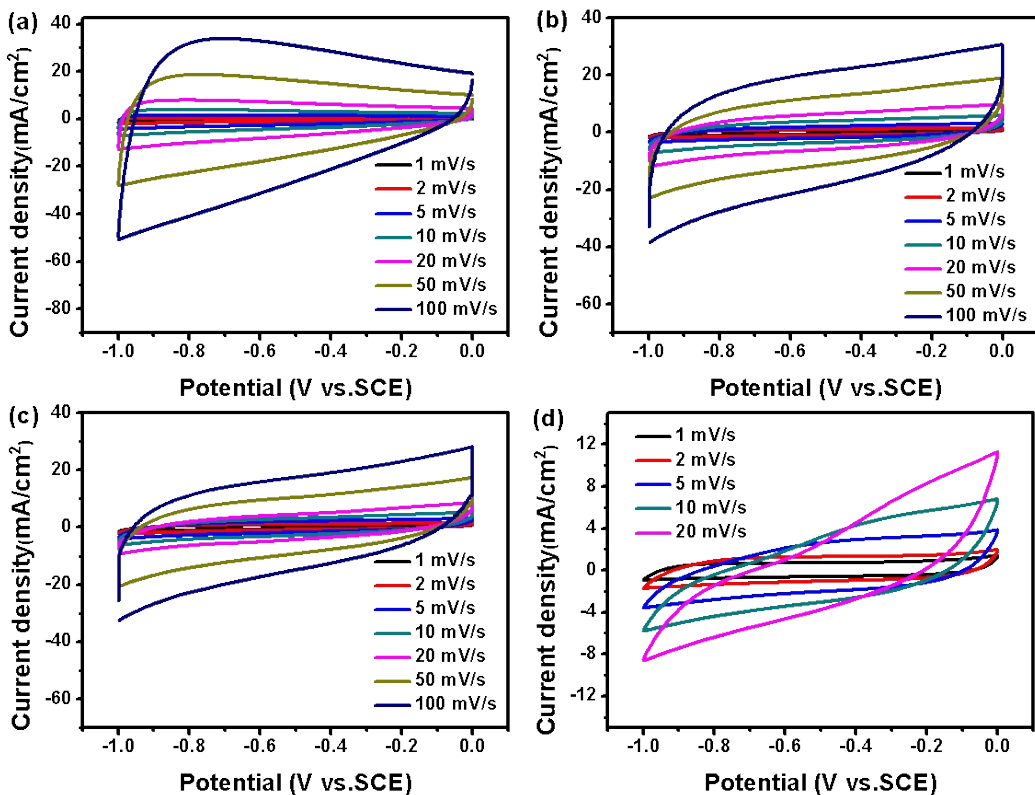


Fig. S10 CV curves of the NPC-600 (a), NPC-800 (b), NPC-900 (c), and PC-700 (d) electrodes at various scan rates.

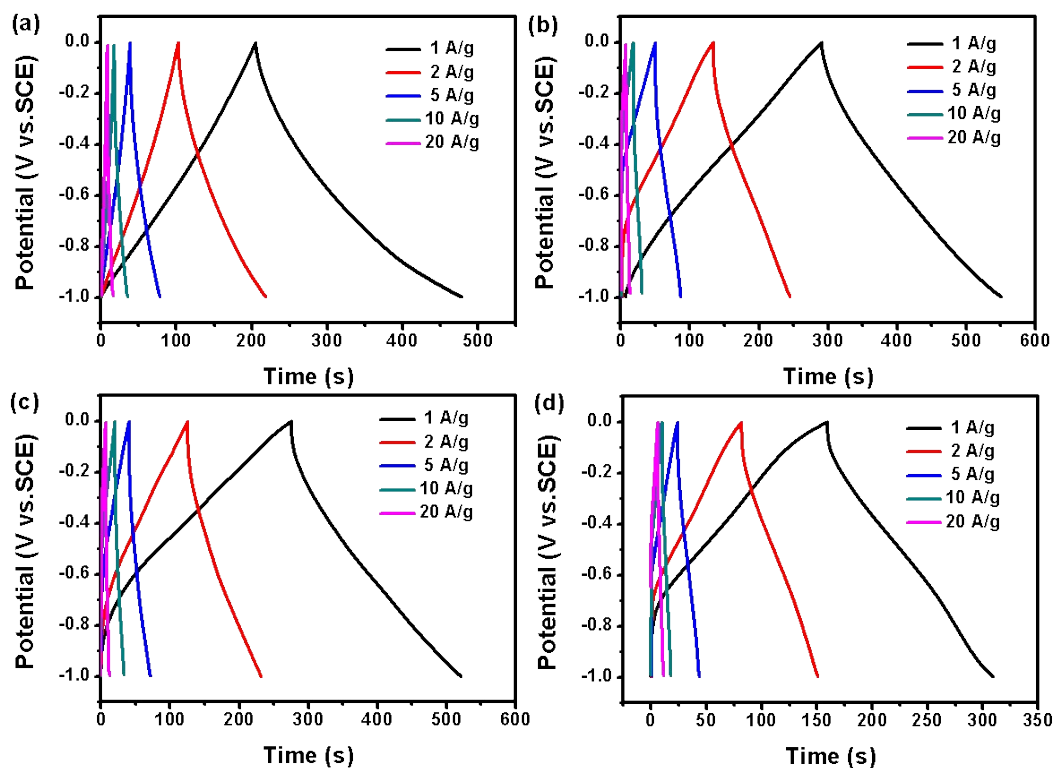


Fig. S11 GCD curves of the NPC-600 (a), NPC-800 (b), NPC-900 (c), PC-700 (d) electrodes at various current densities.

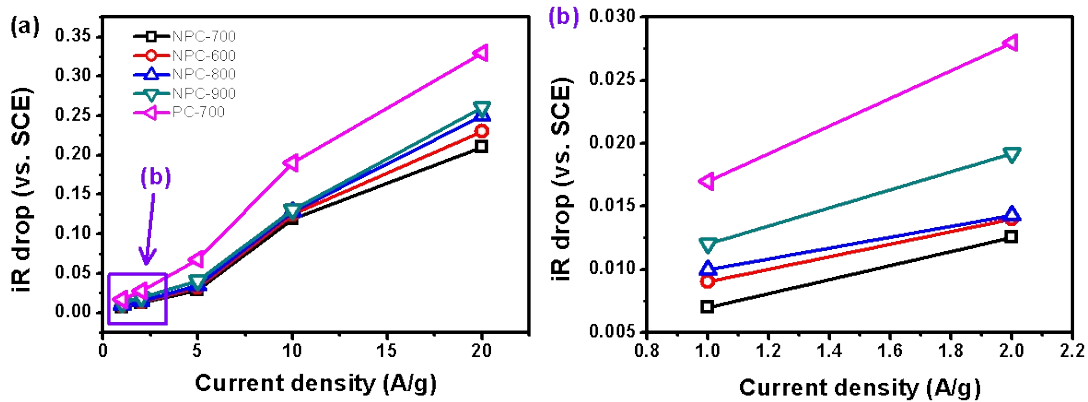


Fig. S12 iR drop of the carbon electrodes measured at different current densities.

Table S3. Relative resistance of NPC samples obtained by fitting the EIS data.

Sample	R_1	R_2	Z_w
NPC-600	12.9	1.1	0.011
NPC-700	12.8	0.8	0.012
NPC-800	13.5	1.3	0.010
NPC-900	13.5	1.4	0.010
PC-700	14.5	1.8	0.010

Table S4. Comparison of electrochemical performance of the carbon electrode from biomass precursors.

Carbon Precursor	C_s (F g ⁻¹)	Measurement Condition	Electrolyte	Ref.
Broad bean shells	202	0.5 A g ⁻¹	6 M KOH	4
Silk	242	0.1 A g ⁻¹	EMIMBF ₄	5
Corn cob	221	1 A g ⁻¹	0.5 M H ₂ SO ₄	6
Carrageenan	230	1 A g ⁻¹	6 M KOH	7
Auricularia	340	1 A g ⁻¹	6 M KOH	8
Enteromorpha prolifera	210	3 A g ⁻¹	6 M KOH	9
Fungi	158	0.1 A g ⁻¹	TEABF ₄	10
Rice Bran	300	1 A g ⁻¹	6 M KOH	11
Protein	320	1 A g ⁻¹	1 M H ₂ SO ₄	12
Human hair	340	1 A g ⁻¹	6 M KOH	13
Shaddock peels	321.7	1 A g ⁻¹	6 M KOH	This work

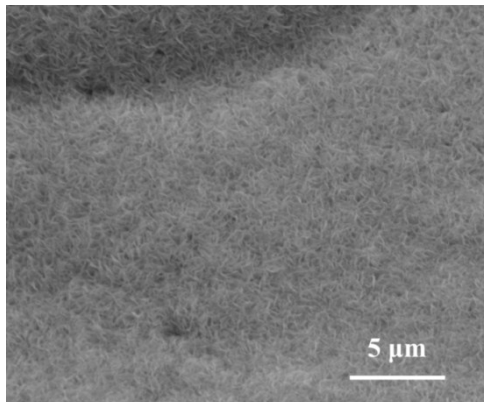


Fig. S13 SEM image of MnO₂ deposited on Ni foam.

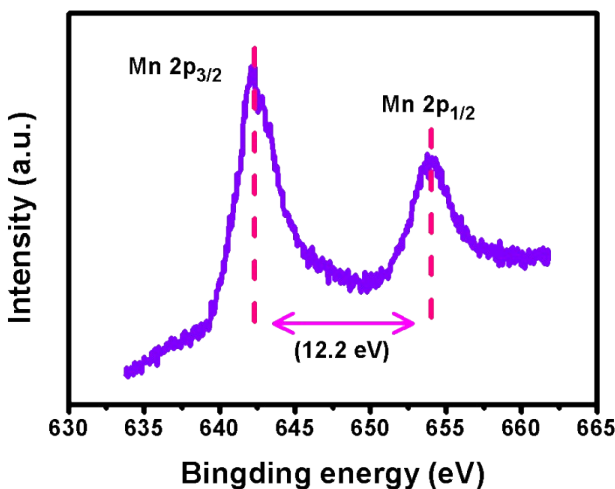


Fig. S14 Mn 2p spectrum of MnO_2 .

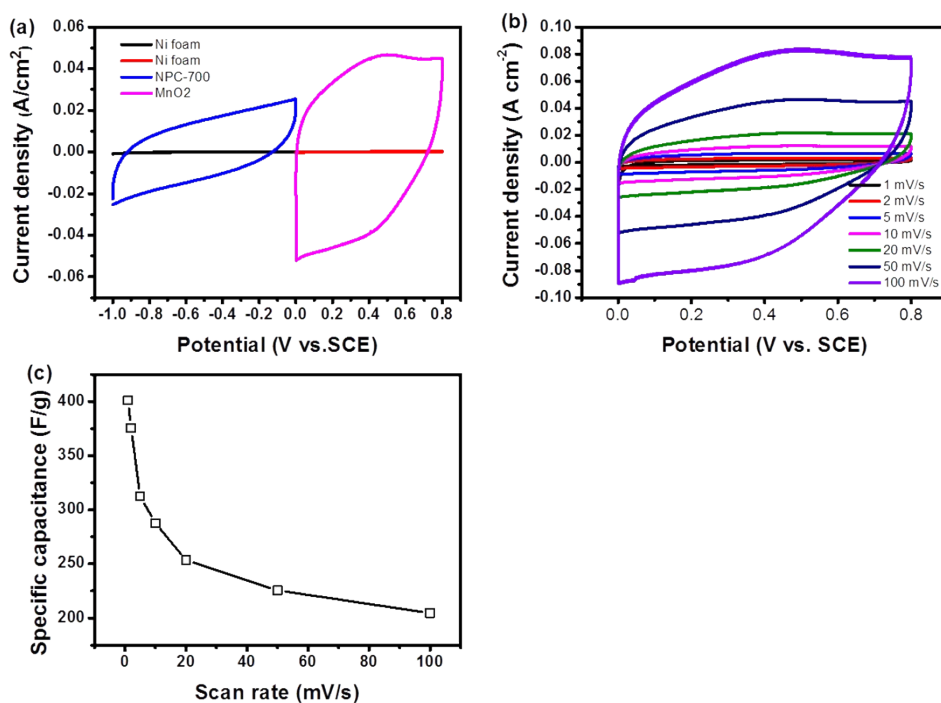


Fig. S15 (a) Comparative CV curves of NPC-700 and MnO_2 electrodes at a scan rate of 50 mV s⁻¹. (b) CV curves of the MnO_2 electrode at various scan rates. (c) Specific capacitance of MnO_2 electrode calculated from CV curves as a function of scan rate.

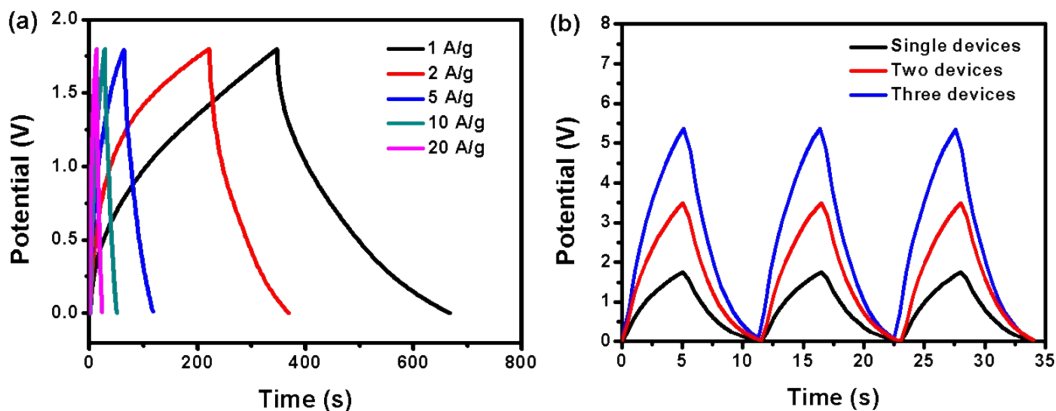


Fig. S16 (a) GCD curves of $\text{MnO}_2/\text{NPC-700}$ ASC at different current densities. (b) GCD curves collected at a current density of 30 A g^{-1} for a single solid-state $\text{MnO}_2/\text{NPC-700}$ ASCs and tandem devices where two and three SC units are connected in series.

References

- 1 G. X. Zhao, J. X. Li, L. Jiang, H. L. Dong, X. K. Wang and W. P. Hu, *Chem. Sci.*, 2012, **3**, 433.
- 2 T. Zhai, S. L. Xie, M. H. Yu, P. P. Fang, C. L. Liang, X. H. Lu., Y. X. Tong, *Nano Energy*, 2014, **8**, 255.
- 3 S. Gao, Y. F. Sun, F. C. Lei, L. Liang, J. W. Liu, W. T. Bi, B. C. Pan, Y. Xie, *Angew. Chem. Int. Ed.*, 2014, **53**, 12789.
- 4 G. Y. Xu, J. P. Han, B. Ding, P. Nie, J. Pan, H. Dou, H. S. Li, *Green Chem.*, 2015, **17**, 1668.
- 5 J. H. Hou, C. B. Cao, F. Idrees, X. L. Ma, *ACS Nano*, 2015, **9**, 2556.
- 6 M. Genovese, J. H. Jiang, K. Lian, N. Holm, *J. Mater. Chem. A*, 2015, **3**, 2903.
- 7 Y. Fan, X. Yang, B. Zhu, P. F. Liu, H. T. Lu, *J. Power Sources*, 2014, **268**, 584.
- 8 C. L. Long, X. Chen, L. L. Jiang, L. J. Zhi, Z. J. Fan, *Nano Energy*, 2015, **12**, 141.
- 9 Y. Gao, W. L. Zhang, Q. Y. Yue, B. Y. Gao, Y. Y. Sun, J. J. Kong, P. Zhao, *J. Power Sources*, 2014, **270**, 403.
- 10 J. C. Wang, Q. Liu, *RSC Adv.*, 2015, **5**, 4396.
- 11 J. Hou, C. Cao, F. Idrees, B. Xu, X. Hao, W. Lin, *Sci. Rep.*, 2014, **4**, 7260.
- 12 Z. Li, Z. W. Xu, X. H. Tan, H. L. Wang, C. M. B. Holt, T. Stephenson, B. C. Olsen, D. Mitlin, *Energy Environ. Sci.*, 2013, **6**, 871.
- 13 W. J. Qian, F. X. Sun, Y. H. Xu, L. H. Qiu, C. H. Liu, S. D. Wang, F. Yan, *Energy Environ. Sci.*, 2014, **7**, 379.